Chemical short-range order in complex concentrated alloys

Wei Chen,* Lin Li, Qiang Zhu, and Houlong Zhuang

Complex concentrated alloys (CCAs) have drawn immense attention from the materials research community and beyond. Because the vast compositional and structural degrees of freedom in CCAs can lead to novel properties (e.g., structural and functional) with a wide range of applications, the structure–property relationships of CCAs are of critical interest. One salient feature in the atomic structures of CCAs is the presence of chemical short-range ordering (CSRO). Understanding the roles of CSRO on properties, especially phase stability, requires joint efforts from experimental and computational approaches. In this article, we first briefly survey the most recent experimental efforts in identifying and characterizing CSRO of various CCAs. We then focus on the theoretical and computational techniques that have been deployed to investigate the CSRO effects. These computational methods include density functional theory (DFT), molecular dynamics (MD), and statistical mechanics methods such as cluster expansions and machine learning methods such as creating transferable interatomic potentials. Finally, we outline the challenges and future directions of CSRO research in CCAs.

Introduction

Complex concentrated alloys (CCAs), or high-entropy alloys (HEAs), demonstrate four fundamental effects: the high configurational entropy effect, the sluggish diffusion effect, the lattice distortion effect, and the "cocktail" effect.[1] These effects influence various aspects of CCAs, such as their thermodynamics, kinetics, structures, and properties. However, the presence of chemical short-range order (CSRO), which refers to a chemical preference-induced ordered arrangement of atoms over short atomic distances, adds an additional level of complexity, which can significantly impact the structure–property relationships of CCAs.

CSRO can stabilize phases in CCAs by reducing the mixing enthalpy, contrary to the high mixing enthalpy that generally provides a driving force for phase separation. Meanwhile, CSRO reduces the strain energy caused by lattice mismatch and can mitigate one of the four core effects of CCAs, the lattice distortion effect. CSRO also affects other thermodynamic properties, particularly the melting temperature. In a recent theoretical study,[2] a combination of molecular dynamics (MD) and Monte Carlo (MC) simulations was employed to investigate the impact of elemental concentration, CSRO, and atomic segregation on the melting temperature of the $AlCoFeNiCu_x$ CCAs with three different concentrations of Cu ($x=0$, 0.5, and 1). It was found that, as the concentration of Cu increases, the melting temperature decreases due to the increased occurrence of CSRO and atomic segregation with phase boundary. This melting temperature dependence on the concentration of Cu is consistent with the experimental observed trend.

CSRO can also impact the mechanical properties of CCAs. In fact, CSRO strengthening serves as an important mechanism to enhance the strength of CCAs. For instance, Zhang et al. have shown that it is possible to alter the mechanical properties of CCAs by modifying the degree of CSRO through thermomechanical processing.[3] In their study, the mechanical properties of the alloys were assessed through bulk tensile tests, nanoindentation, and a diffraction contrast scanning transmission electron microscope (TEM) to determine the influence of CSRO. The energy-filtered TEM was used, allowing for the observation of CSRO domains in a CrCoNi, which agrees with the previous theoretical predictions. Moreover, a direct correlation was established between the presence of CSRO domains and improved mechanical properties. As another example, through a combination of various

Wei Chen, Department of Mechanical, Materials, and Aerospace Engineering, Illinois Institute of Technology, Chicago, USA; wchen66@iit.edu
Lin Li, School for Engineering of Matter, Transport and Energy, Arizona State University, Tempe, USA; lin.li.10@asu.edu
Qiang Zhu, Department of Physics and Astronomy, University of Nevada, Las Vegas, USA; qiang.zhu@unlv.edu
Houlong Zhuang, School for Engineering of Matter, Transport and Energy, Arizona State University, Tempe, USA; zhuanghl@asu.edu
*Corresponding author
doi:10.1557/s43577-023-00575-8

computational simulations, including MC and MD simulations, and density functional theory (DFT) calculations, the CSRO was predicted to be present in a CoCuFeNiPd CCA and enhances both the ultimate strength and ductility.[4] This synergistic enhancement is through the formation of face-centered-cubic-preferred (fccp) and body-centered-cubic-preferred (bccp) clusters. Specifically, the fccp and bccp clusters enhance the strength and ductility, respectively. At the atomic scale, CSRO disrupts favorable bonding to increase the resistance for dislocations to slip (**Figure 1**).

Moreover, CSRO can also impact the functional properties of CCAs, including magnetic properties of CCAs. For example, the presence of CSRO in the $FeCoNi(AlSi)_x$ alloys alters the atomic nearest-neighbor environment, resulting in a decrease in the magnetic moments of the magnetic elements.[5] By accounting for the effect of CSRO, the saturation magnetizations (i.e., the maximum magnetization) obtained from theoretical calculations align well with the experimental values.

Although CSRO can have significant effects on the properties of CCAs, there are both computational and experimental challenges in understanding and controlling CSRO. To perform computational simulations such as DFT calculations on the disordered atomic structure of a CCA, suitable structural models are required to model the CSRO in a CCA. Two approaches are commonly used to model random CCAs: (1) randomly placing atoms of various elements in fixed lattice sites of a large supercell, and (2) creating a special quasi-random structure (SQS)[6] whose correlation functions match those of truly random alloys. However, it is important to note that these structures are just a "snapshot" of the disordered CCA, and multiple calculations must be performed on many snapshots to obtain a statistical average of the property being studied, such as total energies. An alternative approach is the virtual crystal approximation (VCA),[7] which uses an averaged potential from mixing elemental potentials to describe CCAs. Compared to regular DFT calculations of large supercells, the VCA method performs calculations on significantly smaller unit cells, making it much simpler and less computationally expensive. However, CSRO as well as local distortions are neglected at the VCA level in the theory and therefore cannot replicate all four core effects of CCAs. Experimentally, detecting and measuring the relatively weak SRO diffraction signal is a challenging task.[3] Compared to the long-range lattice diffraction signal, the diffraction contrast originating from the relatively minor differences in atomic scattering factors between the constituent elements of CSRO is naturally faint. Additionally, if structural information such as extended x-ray absorption fine structure (EXAFS) data are available, experimental data can be used to reveal the pair correlation functions among the constituent elements of a CCA. A structure-inversion algorithm can also be developed to reproduce the EXAFS data in a simulation supercell, which can capture the statistical, structural, and electrical characteristics in CCAs, bypassing many time-consuming calculations.

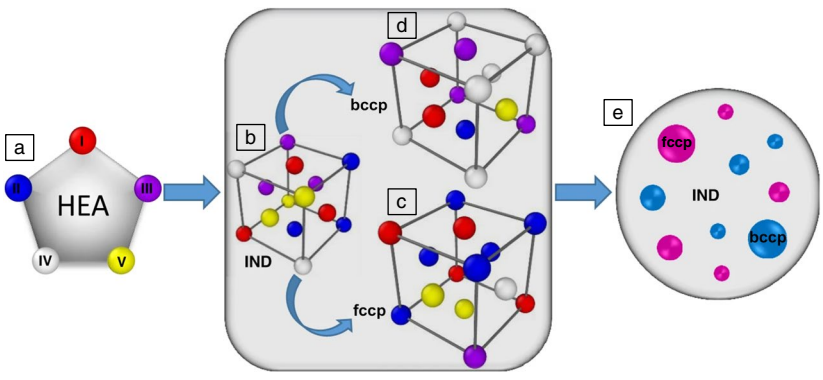

Figure 1. (a) Design of a complex concentrated alloy with five elements (I, II, III, IV, and V). Formation of (b) IND, (c) face-centered-cubic-preferred (fccp), and (d) body-centered-cubic-preferred (bccp) clusters via short-range ordering. (e) The cluster indifferent to fcc/bcc phase (i.e., IND clusters) serve as a matrix with the fccp clusters serving as hard fillers to enhance the strength and bccp clusters act as (plastically) soft fillers to increase the ductility.[4] HEA, high-entropy alloy.

Experimental characterizations of CSRO

CSRO is usually analyzed using a range of techniques, including x-ray diffraction, neutron diffraction, and transmission electron microscopy (TEM). However, there are many challenges in characterizing the CSRO in CCAs due to their unique characteristics. First, in an *N*-component CCA system, there are $N(N\text{-}1)/2$ unlike and *N*-like atomic pairs. Identifying these specific atomic pairs experimentally requires sufficient contrast, such as differences in atomic size or mass, between the atoms. Second, the CSRO typically emerges on a sub-nanometer scale, which requires precise imaging of atomic rearrangements with a spatial resolution below 1 nm. These challenges highlight the need for advanced analytical methods to fully understand the CSRO of CCAs.

The conventional method for analyzing CSRO is through single-crystal diffraction.[8] CSRO produces characteristic diffuse scattering, which can be quantitatively determined by x-ray and neutron diffraction, enabling the identification of atomic pair correlations. However, for CCAs, high-precision techniques are often required to enhance the scattering contrast.[9,10] For example, when examining the local structure of NiCoCr with neutron and x-ray diffraction, pair distribution function analysis was unable to distinguish the bond length and variations of pairs between atomic species due to the similarity of atomic size and scattering properties. Nonetheless, EXAFS analysis revealed a subtle difference in the position of the first peak, indicating that Cr tends to bond with Ni and Co.[9] Additionally, the presence of CSRO in CrFeCoNi was established through diffuse x-ray scattering by exploiting

variations of scattering contrast close to the absorption edges of each constituent.[10] However, interpreting the diffuse scattering from samples can be challenging, and obtaining detailed pairwise correlations of chemical order requires large-box modeling using either *ab initio* MD simulations or reverse Monte Carlo (RMC) refinement techniques.[9–12] Indirect, volume-averaged bulk experimental techniques leave much room for interpretation of how CSRO proceeds at the atomic scale.

Directly imaging CSRO with the atomic resolution in CCAs remains a difficult task when using a TEM due to the lack of strong elemental contrast. However, recent advances in characterization and analysis techniques such as scanning transmission nanobeam diffraction with energy filtering, high-angle annular dark-field (HAADF) imaging, and high-resolution energy-dispersive x-ray spectroscopy have started to provide promising results in a few CCA systems.[3,13–15] **Figure 2** displays the evidence of CSROs revealed in a fcc CrCoNi concentrated solution.[15] As shown in Figure 2a, the HAADF image captured using the [112] zone axis revealed the extra superlattice reflections in the fast Fourier transform (FFT) pattern, indicating the presence of CSRO. The inverse FFT image (Figure 2b) demonstrated that the interplanar spacing of the CSRO was twice the interplanar spacing of the corresponding normal fcc plane. Further nanobeam diffraction experiments using the [112] zone axis (Figure 2c) provided additional evidence of CSRO, improving the signal-to-noise ratio significantly. In the dark-field TEM, taken using the extra disks, CSRO regions are visible and are typically less than 1 nm in size, occupying approximately 20% of the total area in these images (Figure 2d). Additionally, using energy-dispersive x-ray spectroscopy (EDS) mapping (Figure 2e–f) based on HAADF imaging provided detailed atomic arrangement constituting CSROs. Notably, the Cr-enriched planes alternate with those enriched in Co and/or Ni, with alternating chemical occupancy extending across only a few planes, indicating chemical short-to-medium range order.

The suite of advanced electron microscopy tools has provided important details of atomic structures in CCAs, shedding a light on the evolution of CSRO during thermomechanical processing[3,15] and establishing connections between CSRO and CCA properties.[3] However, a quantitative determination

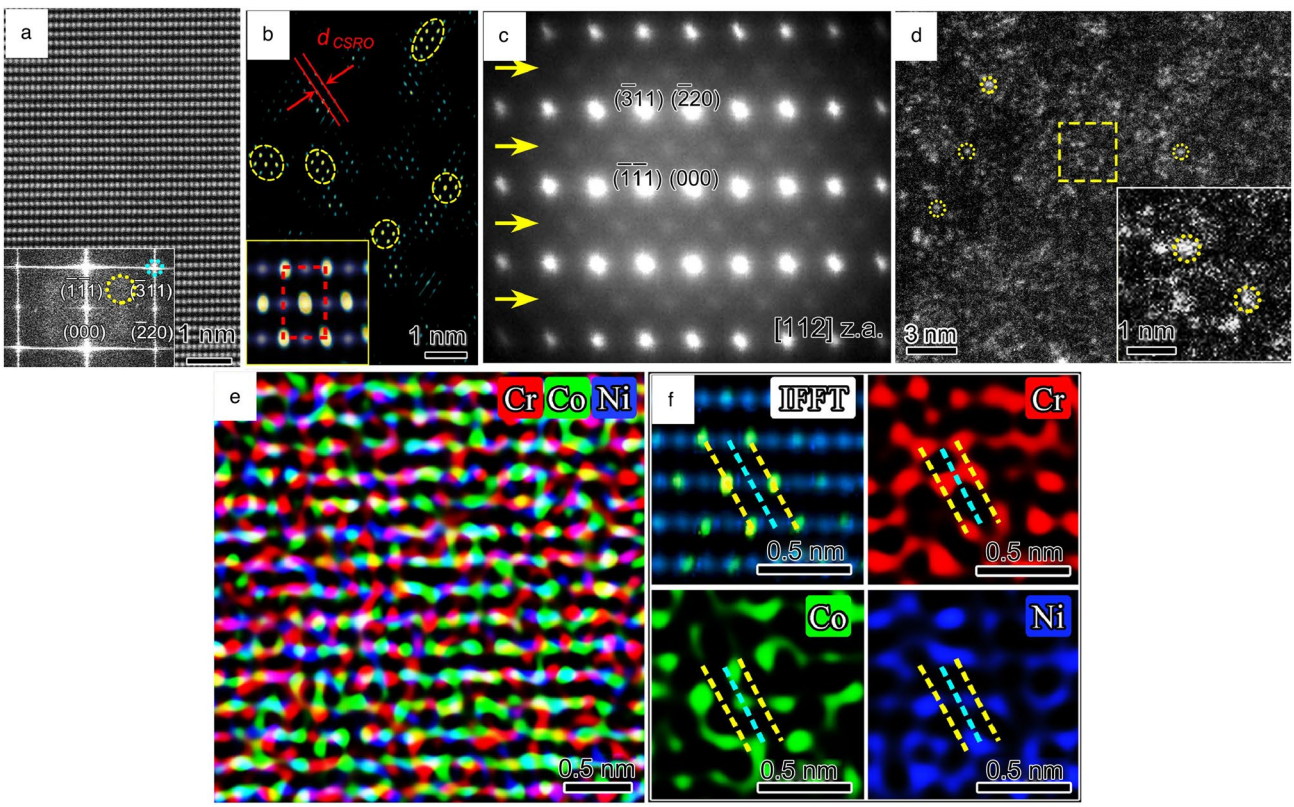

Figure 2. Evidence of chemical short-range order (CSRO) in face-centered-cubic (fcc) CrCoNi annealed at 600°C from electron microscope. (a) High-angle annular dark-field lattice image of the fcc phase with the [112] zone axis. The inset shows the corresponding fast Fourier transform (FFT) pattern, where extra diffuse reflections labeled by a yellow circle indicate the presence of CSRO. (b) Inverse FFT images of CSRO regions revealing the interplanar spacing of CSROs is twice that of the corresponding normal fcc plane. (c) Nanobeam diffraction pattern with the [112] zone axis showing arrays of extra diffuse reflections pointed out by arrows. (d) Energy-filtered dark-field transmission electron microscope image taken using extra diffuse disks. The inset highlights some coherently diffracting CSROs. (e) Energy-dispersive x-ray spectroscopy map showing the distribution of Cr, Co, and Ni. (f) Inverse FFT of a specific CSRO region (upper-left) and close-up maps of Cr, Co, and Ni, respectively, for this region. All data from Reference 15.

of CSRO and local atomic structures is still needed, and it is unclear whether these observations support theory-predicted CSRO.[16,17] Recent work has demonstrated a data-driven electron diffraction approach[18] that can overcome the limitations of traditional diffuse scattering analysis with orders of magnitude improvement in spatial resolution. Nonetheless, although TEM provides two-dimensional through-thickness projections of CSRO, it limits the measurement of the size and morphology of CSRO domains in three-dimensional (3D) space.

CSRO in CCAs can create local atomic-level chemical clustering of like elements and result in chemical fluctuations within the material. Atom probe tomography (APT) is a powerful technique capable of providing 3D mapping of elemental heterogeneities, in principle, at the subnanometer scale with high sensitivity for similar elements.[19] With near-atomic spatial resolution and high analytical sensitivity, APT can help quantify the size and morphology of CSRO domains in 3D. In the CrCoNi sample, for example, closer inspection of APT data using partial radial distribution function (RDF) analysis shows evidence of Ni clustering extending to a few nanometers in radius, with negative Ni–Cr and Co–Cr correlations, consistent with electron diffraction measurements.[18,20] However, the spatial resolution of the APT technique currently prevents precise imaging of atomic ordering, particularly in domains below 1 nm in diameter. Advanced analysis of APT data using machine learning algorithms could help overcome this limitation and improve the characterization of CSRO in CCAs.

Obtaining accurate and quantitative information about CSROs is crucial for establishing the connection between CSROs and properties of CCAs. To achieve this, the improvement of scattering contrast among the constituents remains a key challenge, particularly for scattering techniques such as x-ray, neutron, and electron diffraction. By combining advanced modeling methods with scattering techniques, high-resolution EDS and APT characterization can provide elemental mapping with a high level of detail. Although most experimental studies on CSROs in CCAs have focused on fcc lattices, more research is needed to investigate other types of structures, such as bcc and hexagonal close-packed (hcp) systems, in order to gain a more comprehensive understanding of the relationship between CSROs and CCA properties.

Computational predictions of CSRO

The computational study of CSRO has a long history for binary alloys. CSRO can be quantified by the Warren–Cowley parameter: $\alpha_i = 1 - P_B(i)/x_B$, where $P_B(i)$ is the probability of B atoms on the i*th* nearest-neighbor shell about an A atom, and x_B is the concentration of B atoms of the alloy.[21] In a random alloy, $\alpha_i = 0$. CSRO exhibits as clustering of *like* atoms, $\alpha_i < 0$, or ordering of *unlike* atoms, $\alpha_i > 0$. The spatial correlation of CSRO atoms indicates *preferential interactions* between certain species in the alloy, which is known to affect the phase stability of solid solutions,[22] mechanical properties,[23] and even electronic properties.[24] Experimentally, the Fourier transform of the diffuse x-ray or neutron,[16,25–27] scattering intensity can measure CSRO parameters.[21] Computationally, first-principles methods with statistical mechanical techniques have also successfully verified SRO in many binary systems.[24,28,29]

Despite the importance in alloys, CSRO has been largely ignored in the studies of CCAs until recently.[17] CSRO reduces the configurational entropy ΔS^{conf}, but it can also stabilize solid solutions by reducing the mixing enthalpy.[30] However, it is technically challenging to determine CSRO in CCAs. For computations, without knowing the CSRO *a priori*, SQS cannot directly predict CSRO. The Korringa–Kohn–Rostoker (KKR) Green's function with coherent-potential approximation (CPA) predicts CSRO, but it does not consider lattice distortion.[16] Statistical mechanical methods that combine MC simulations with *ab initio* MD[31,32] or first-principles cluster expansions (CEs) are more rigorous for CSRO in CCAs. These calculations are expensive, but recent results on refractory CCAs are encouraging.[33,34] The relationship between CSRO and lattice distortion is accessible from these methods.[35]

From a computational point of view, CSRO can be directly modeled by MC algorithms. However, this is difficult to achieve in MC algorithms that are based on the canonical ensemble. To address this challenge, Sadigh et al. recently developed an algorithm that effectively models the equilibrium properties of phase-segregated multicomponent systems in the variance-constrained semi-grand-canonical (VC-SGC) ensemble.[36] This algorithm incorporates transmutation moves with MD steps, allowing for the inclusion of structural relaxations and thermal vibrations in large-scale alloy models. In the past decade, this type of hybrid simulation was mostly carried out together with the classical force fields such as the embedded-atom method (EAM). For instance, Li et al. applied the EAM potential to study the NiCoCr alloy and found that the CSRO changes with alloy processing conditions.[37] The variety of CSRO can effectively change the ruggedness of the energy landscape and raise the activation barriers governing dislocation activities. The impacts of CSRO on the properties of CCAs have been extensively studied using EAM potentials, such as strengthening,[38] solution hardening,[39] dislocation motion,[40] and ductility.[4]

Despite the popularity of EAM potential in CCA modeling, these potentials were typically fitted mainly to elemental properties and their performances deem to become worse when scaled to multicomponent alloys. With an efficient predictive energy model, the CSRO can be more reliably predicted from MC simulations.[41] For CCAs, reliable empirical potentials are not readily available. Widely used in binary alloys, first-principles CE offers a rigorous statistical mechanics approach to generate accurate energy models using a lattice model.[42–44] CE can determine the stable atomic configuration with CSRO for a lattice system. In CE, an atomic configuration σ is described by pseudospins for the lattice system. The CE predicts the energy E (or any other configurational-dependent property) for σ as the additions of "interactions"

from clusters f of atoms, such as points, pairs, and triples. $E(\sigma) = \sum_f m_f J_f \langle \Gamma_{f'}(\sigma) \rangle_f = \sum_f J_f \Pi_f(\sigma)$, where m_f is the multiplicity of f, $\Gamma_f(\sigma)$ are cluster functions that form an orthogonal basis for the function of the configurational space, $\Pi_f(\sigma)$ is the structural correlation function for f, J_f are the effective cluster interactions (ECIs) that are expansion coefficients for a set of clusters derived from first principles.[45,46] When *all* clusters are included, the CE Hamiltonian is *exact* and considers atomic relaxations.[47] In practice, the expansion is truncated to include clusters that are significant in predicting E.[44] The choice of clusters is vital to the predictive power of CE. Cross-validations can reduce under- and overfitting,[48] but selecting a set of clusters from a large number of candidates is still an *NP*-hard problem with a daunting complexity. Finding the best set of clusters is possible for binary alloys,[49,50] but it is challenging for CCAs due to the combinatorial explosion in the number of clusters. The CE method has been applied to predict the CSRO in the MoNbTaVW CCA, predicting the strongest CSRO pair to be the first nearest-neighbor Mo–Ta pair, consistent with the high stability of the B2 Mo–Ta binary system.[54]

Integrating DFT structural optimization or *ab initio* MD with MC simulation is another popular approach to study CSRO in CCAs. These methods are computationally expensive, but they circumvent the difficulties in constructing accurate energy models for CCA systems. Hybrid MC–MD simulations have evaluated the temperature-dependent CSRO in the MoNbTaW CCA, revealing the B2 ordering between mixed (Nb, Ta) and (Mo, W) sites near room temperatures.[32] The effects of CSRO on the stacking-fault energies of CrCoNi were investigated in a study using DFT-based MC simulations.[17] The DFT-predicted stacking-fault energy for a completely random CrCoNi yields negative values, in contradiction to measured finite dislocation width. However, the DFT-based MC simulations found the stacking-fault energies are highly tunable for the CCA, giving increasingly positive stacking-fault energies with a higher degree of CSRO (**Figure 3**). Because the stacking faults in CCAs are correlated with transformation-induced plasticity,[51] the predicted CSRO can potentially be tuned to tailor the mechanical behavior of CCAs.

In recent years, machine learning methods have been widely applied in materials modeling.[52,53] The main idea of machine learning in atomistic modeling is to represent each local atomic environment in the solid by a set of symmetry-invariant high dimensional vectors.[54,55] Consequently, the machine learning potentials (MLPs) are trained by minimizing the cost function to deliberately attune the model to describe the DFT data. The cost of atomistic simulation is orders of magnitude lower than the quantum mechanical simulation, allowing the system to be scaled up to 1 million atoms. To date, several regression techniques, including neural networks (NNs),[53,56] Gaussian process regression,[57] and line regression,[55,58] are popular choices for MLP development. Many applications based on different MLP models have shown that the machine learning approach works remarkably well in various atomistic simulations.[59,60] These encouraging results show the promise of using MLP to resolve the dilemma of compromising accuracy and cost for traditional models based on DFT or classical force fields.

In particular, several MLP models have been developed to investigate the CCA systems.[61–64] Kostiuchenko et al. first demonstrated a high efficiency and performance of the MTP-derived MLP approach on the prototype bcc NbMoTaW CCA, as shown on a set of benchmarked properties, including phase stability, phase transitions, and CSRO as well.[61] Li et al. also developed another MLP on the same system and investigated both single- and polycrystalline

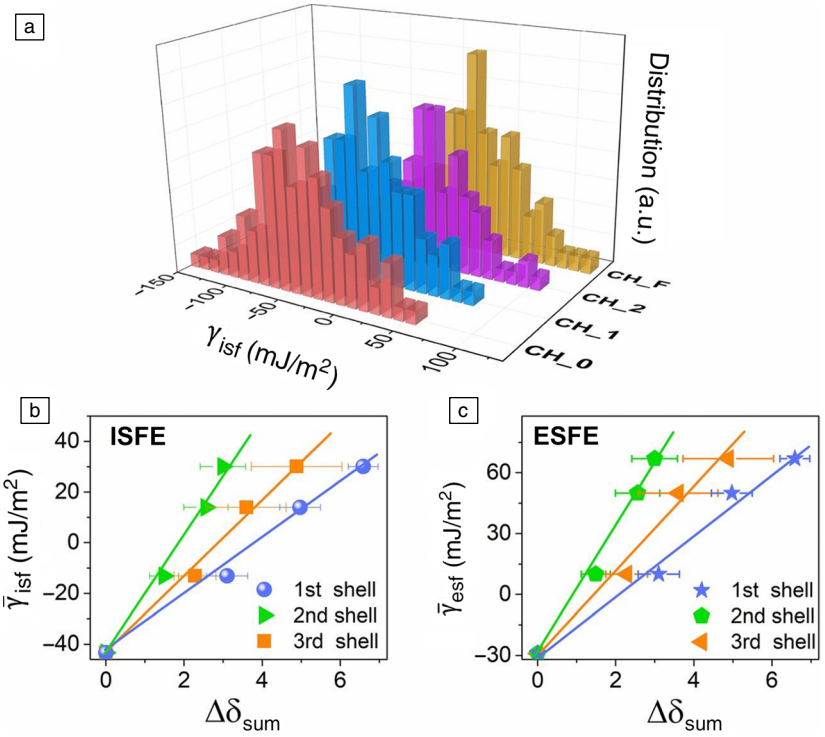

Figure 3. Stacking-fault energy (SFE) in CrCoNi correlates strongly with local chemical ordering. (a) Distribution of intrinsic stacking-fault energy for the CrCoNi alloys in four specific states, which span from random solid solution to the highest degree of chemical ordering extracted from the MC simulations. The average SFEs, (b) intrinsic SFE (ISFE) $\overline{\gamma_{isf}}$, (c) extrinsic SFE (ESFE) $\overline{\gamma_{esf}}$, among those four groups are plotted versus the nonproportional number of local atomic pairs $\Delta\delta_{ij}^{k}$ for the first, second, and third nearest-neighbor shells.[17]

samples to investigate the strengthening mechanism.[62] They found that Nb enrichment of the grain boundary (GB) and intensification of the CSRO can notably enhance the strength of the NbMoTaW CCA over a random solid solution. Furthermore, the same group of authors retrained the MLP based on another descriptor to study the mobilities of screw and edge dislocations over a wide temperature range.[63] According to their results, the mobility of edge dislocations is found to be enhanced by the presence of CSRO, whereas the rate of double-kink nucleation in the motion of screw dislocations is reduced, although this influence of CSRO appears to be attenuated at increasing temperature. More recently, the impacts of CSRO on the elasticity, vibrational modes, plasticity, and strength have also been systematically investigated on both equiatomic and nonequiatomic MoTaNbW quaternaries by the MLP approach, suggesting a wide range of possibilities to tune the mechanical properties of CCA by processing optimization.[64]

Future directions

Studying CSRO is a promising new direction in the research of CCAs. This field requires close collaboration between experimental and computational efforts. Accurate characterization and description of CSRO in CCAs are critical for understanding the correlation between CSROs and CCA properties, as well as for guiding the design of novel CCAs. Furthermore, researchers are also interested in exploring how CSRO affects electron and phonon scattering mechanisms, as this could have a significant impact on the transport properties of CCAs. CSRO has the potential to alter the behavior of phonons and electrons, leading to changes in phonon and electron scattering that could either increase or decrease the scattering of both electrons and phonons, thereby affecting both types of transport behavior. This research is particularly significant as there is growing interest in developing thermoelectric CCAs that exhibit high electrical conductivity and low thermal conductivity.[65,66] For instance, recent studies have investigated the impact of complex short-range order on the electrical and thermal transport properties of CCAs. Some CCAs, such as CoNiCr, have received particular attention for their CSCO. However, many other CCAs remain relatively unexplored. Also, most of the existing research on CSROs has been conducted through computational studies, so there is a need for experimental studies to validate these predictions. Overall, the emergence of CSRO is a natural feature of many CCAs, offering a unique opportunity for managing the degree of CSRO and tailoring a variety of properties for CCA applications. We anticipate an upsurge in investigations into CSRO across diverse CCAs in the foreseeable future, as researchers delve deeper into this fascinating characteristic and unlock its immense potential for CCA design.

Acknowledgments

W.C. acknowledges the support by the National Science Foundation (NSF) (No. DMR-1945380). L.L. acknowledges the funding support provided by NSF (Grant No. DMR-2104656) and the National Aeronautics and Space Administration (NASA), Alabama EPSCoR (Contract No. 80NSSC21M0176). Q.Z. acknowledges the support from the US Department of Energy, Office of Science, Office of Basic Energy Sciences, Theoretical Condensed Matter Physics program, DOE Established Program to Stimulate Competitive Research under Award No. DE-SC0021970. H.Z. acknowledges the support by NSF (Grant No. DMR-2239216).

Funding

National Science Foundation, DMR-1945380, W.C., DMR-2104656, L.L., DMR-2239216, H.Z., National Aeronautics and Space Administration, 80NSSC21M0176, L.L., Office of Science, DE-SC0021970, Q.Z.

Conflict of Interest

On behalf of all authors, the corresponding author states that there is no conflict of interest.

References

1. Y. Zhang, T.T. Zuo, Z. Tang, M.C. Gao, K.A. Dahmen, P.K. Liaw, Z.P. Lu, *Prog. Mater. Sci.* **61**, 1 (2014)
2. S. Chen, T. Wang, X. Li, Y. Cheng, G. Zhang, H. Gao, *Acta Mater.* **238**, 118201 (2022)
3. R. Zhang, S. Zhao, J. Ding, Y. Chong, T. Jia, C. Ophus, M. Asta, R.O. Ritchie, A.M. Minor, *Nature* **581**, 283 (2020)
4. S. Chen, Z.H. Aitken, S. Pattamatta, Z. Wu, Z.G. Yu, D.J. Srolovitz, P.K. Liaw, Y.-W. Zhang, *Nat. Commun.* **12**, 4953 (2021)
5. W. Feng, Y. Qi, S. Wang, *Metals* (Basel) **7**, 482 (2017)
6. A. Zunger, S.-H.H. Wei, L.G. Ferreira, J.E. Bernard, *Phys. Rev. Lett.* **65**, 353 (1990)
7. L. Bellaiche, D. Vanderbilt, *Phys. Rev. B Condens. Matter Mater. Phys.* **61**, 7877 (2000)
8. J.M. Cowley, *Phys. Rev.* **77**, 669 (1950)
9. F.X. Zhang, S. Zhao, K. Jin, H. Xue, G. Velisa, H. Bei, R. Huang, J.Y.P. Ko, D.C. Pagan, J.C. Neuefeind, W.J. Weber, Y. Zhang, *Phys. Rev. Lett.* **118**, 205501 (2017)
10. B. Schönfeld, C.R. Sax, J. Zemp, M. Engelke, P. Boesecke, T. Kresse, T. Boll, T. Al-Kassab, O.E. Peil, A.V. Ruban, *Phys. Rev. B.* **99**, 014206 (2019)
11. L.J. Santodonato, Y. Zhang, M. Feygenson, C.M. Parish, M.C. Gao, R.J.K. Weber, J.C. Neuefeind, Z. Tang, P.K. Liaw, *Nat. Commun.* **6**, 5964 (2015)
12. L.R. Owen, H.Y. Playford, H.J. Stone, M.G. Tucker, *Acta Mater.* **115**, 155 (2016)
13. Q. Ding, Y. Zhang, X. Chen, X. Fu, D. Chen, S. Chen, L. Gu, F. Wei, H. Bei, Y. Gao, M. Wen, J. Li, Z. Zhang, T. Zhu, R.O. Ritchie, Q. Yu, *Nature* **574**, 223 (2019)
14. X. Chen, Q. Wang, Z. Cheng, M. Zhu, H. Zhou, P. Jiang, L. Zhou, Q. Xue, F. Yuan, J. Zhu, X. Wu, E. Ma, *Nature* **592**, 712 (2021)
15. L. Zhou, Q. Wang, J. Wang, X. Chen, P. Jiang, H. Zhou, F. Yuan, X. Wu, Z. Cheng, E. Ma, *Acta Mater.* **224**, 117490 (2022)
16. P. Singh, A.V. Smirnov, D.D. Johnson, *Phys. Rev. B* **91**, 224204 (2015)
17. J. Ding, Q. Yu, M. Asta, R.O. Ritchie, *Proc. Natl. Acad. Sci. U.S.A.* **115**, 8919 (2018)
18. H.-W. Hsiao, R. Feng, H. Ni, K. An, J.D. Poplawsky, P.K. Liaw, J.-M. Zuo, *Nat. Commun.* **13**, 6651 (2022)
19. B. Gault, A. Chiaramonti, O. Cojocaru-Mirédin, P. Stender, R. Dubosq, C. Freysoldt, S.K. Makineni, T. Li, M. Moody, J.M. Cairney, *Nat. Rev. Methods Primers* **1**, 51 (2021)
20. K. Inoue, S. Yoshida, N. Tsuji, *Phys. Rev. Mater.* **5**, 085007 (2021)
21. J.M. Cowley, *Phys. Rev.* **120**, 1648 (1960)
22. J.D. Althoff, D.D. Johnson, F.J. Pinski, J.B. Staunton, *Phys. Rev. B* **53**, 10610 (1996)
23. C. Varvenne, G.P.M. Leyson, M. Ghazisaeidi, W.A. Curtin, *Acta Mater.* **124**, 660 (2016)
24. K. Mäder, A. Zunger, *Phys. Rev. B* **51**, 10462 (1995)
25. T.R. Welberry, *Metall. Mater. Trans. A* **45**, 75 (2013)
26. T.R. Welberry, *Rep. Prog. Phys.* **48**, 1543 (1985)
27. C.B. Walker, D.T. Keating, *Phys. Rev.* **130**, 1726 (1963)
28. A. Van der Ven, G. Ceder, *Phys. Rev. B* **71**, 54102 (2005)
29. A. Zunger, C. Wolverton, V. Ozolin, V. Ozoliņš, A. Zunger, *Phys. Rev. B* **57**, 4332 (1998)
30. D.B. Miracle, O.N. Senkov, *Acta Mater.* **122**, 448 (2017)
31. R. Feng, P.K. Liaw, M.C. Gao, M. Widom, *NPJ Comput. Mater.* **3**, 50 (2017)
32. M. Widom, W.P. Huhn, S. Maiti, W. Steurer, *Metall. Mater. Trans. A* **45**, 196 (2014)
33. Y. Ma, Q. Wang, C. Li, L.J. Santodonato, M. Feygenson, C. Dong, P.K. Liaw, *Scr. Mater.* **144**, 64 (2018)

34. A. Fernández-Caballero, J.S. Wróbel, P.M. Mummery, D. Nguyen-Manh, *J. Phase Equilib. Diffus.* **38**, 391 (2017)
35. I. Toda-Caraballo, J.S.S. Wróbel, S.L. Dudarev, D. Nguyen-Manh, P.E.J. Rivera-Díaz-del-Castillo, *Acta Mater.* **97**, 156 (2015)
36. B. Sadigh, P. Erhart, A. Stukowski, A. Caro, E. Martinez, L. Zepeda-Ruiz, *Phys. Rev. B* **85**, 184203 (2012)
37. Q.-J. Li, H. Sheng, E. Ma, *Nat. Commun.* **10**, 3563 (2019)
38. E. Antillon, C. Woodward, S.I. Rao, B. Akdim, T.A. Parthasarathy, *Acta Mater.* **190**, 29 (2020)
39. S.I. Rao, B. Akdim, E. Antillon, C. Woodward, T.A. Parthasarathy, O.N. Senkov, *Acta Mater.* **168**, 222 (2019)
40. X. Wang, F. Maresca, P. Cao, *Acta Mater.* **234**, 118022 (2022)
41. A. van de Walle, M. Asta, *Model. Simul. Mater. Sci. Eng.* **10**, 521 (2002)
42. J.M. Sanchez, *Phys. Rev. B* **48**, 14013 (1993)
43. W. Chen, D. Schmidt, W.F. Schneider, C. Wolverton, *Phys. Rev. B* **83**, 075415 (2011). https://doi.org/10.1103/PhysRevB.83.075415
44. D.B. Laks, L.G. Ferreira, S. Froyen, A. Zunger, *Phys. Rev. B* **46**, 12587 (1992)
45. A. van de Walle, *CALPHAD* **33**, 266 (2009)
46. A. Zunger, L.G. Wang, G.L.W. Hart, M. Sanati, *Model. Simul. Mater. Sci. Eng.* **10**, 685 (2002)
47. J.M. Sanchez, F. Ducastelle, D. Gratias, *Phys. A Stat. Mech. Appl.* **128**(1), 334 (1984)
48. A. van de Walle, G. Ceder, *J. Phase Equilib.* **23**, 348 (2002)
49. V. Blum, G.L.W. Hart, M.J. Walorski, A. Zunger, *Phys. Rev. B* **72**, 165113 (2005)
50. O. Levy, G.L.W. Hart, S. Curtarolo, *J. Am. Chem. Soc.* **132**, 4830 (2010)
51. X. Wang, R.R. De Vecchis, C. Li, H. Zhang, X. Hu, S. Sridar, Y. Wang, W. Chen, W. Xiong, *Sci. Adv.* **8**, eabo7333 (2022)
52. Y. Zuo, C. Chen, X. Li, Z. Deng, Y. Chen, J. Behler, G. Csányi, A.V. Shapeev, A.P. Thompson, M.A. Wood, S.P. Ong, *J. Phys. Chem. A* **124**, 731 (2020)
53. H. Yanxon, D. Zagaceta, B. Tang, D.S. Matteson, Q. Zhu, *Mach. Learn. Sci. Technol.* **2**, 027001 (2021)
54. A.P. Bartók, R. Kondor, G. Csányi, *Phys. Rev. B* **87**, 184115 (2013)
55. A.V. Shapeev, *Multiscale Model. Simul.* **14**, 1153 (2016)
56. J. Behler, *Int. J. Quantum Chem.* **115**, 1032 (2015)
57. A.P. Bartók, G. Csányi, *Int. J. Quantum Chem.* **115**, 1051 (2015)
58. A.P. Thompson, L.P. Swiler, C.R. Trott, S.M. Foiles, G.J. Tucker, *J. Comput. Phys.* **285**, 316 (2015)
59. P.A. Santos-Florez, H. Yanxon, B. Kang, Y. Yao, Q. Zhu, *Phys. Rev. Lett.* **129**, 185701 (2022)
60. V.L. Deringer, N. Bernstein, G. Csányi, C. Ben Mahmoud, M. Ceriotti, M. Wilson, D.A. Drabold, S.R. Elliott, *Nature* **589**, 59 (2021)
61. T. Kostiuchenko, F. Körmann, J. Neugebauer, A. Shapeev, *NPJ Comput. Mater.* **5**, 55 (2019)
62. X.-G. Li, C. Chen, H. Zheng, Y. Zuo, S.P. Ong, *NPJ Comput. Mater.* **6**, 70 (2020)
63. S. Yin, Y. Zuo, A. Abu-Odeh, H. Zheng, X.-G. Li, J. Ding, S.P. Ong, M. Asta, R.O. Ritchie, *Nat. Commun.* **12**, 4873 (2021)
64. P. A. Santos-Florez, S.-C. Dai, Y. Yao, H. Yanxon, L. Li, Y.-J. Wang, Q. Zhu, X. Yu, *Acta Mater.* **255**, 119401 (2023)
65. B. Jiang, Y. Yu, H. Chen, J. Cui, X. Liu, L. Xie, J. He, *Nat. Commun.* **12**, 3234 (2021)
66. B. Jiang, Y. Yu, J. Cui, X. Liu, L. Xie, J. Liao, Q. Zhang, Y. Huang, S. Ning, B. Jia, B. Zhu, S. Bai, L. Chen, S.J. Pennycook, J. He, *Science* **371**, 830 (2021) □

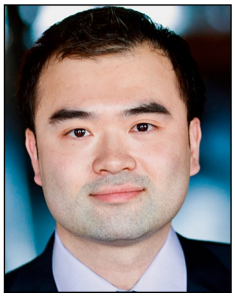

Wei Chen is an associate professor at the Illinois Institute of Technology. He received his PhD degree in materials science and engineering from Northwestern University and has performed his postdoctoral research with the Materials Project at Lawrence Berkeley National Laboratory. His research focuses on accelerated materials discovery integrating atomistic modeling and data-driven methods. He is a recipient of the National Science Foundation CAREER Award, National Energy Research Scientific Computing Center Early Career Award for High Impact Scientific Achievement, and BHP Billiton Fellowship. Chen can be reached by email at wchen66@iit.edu.

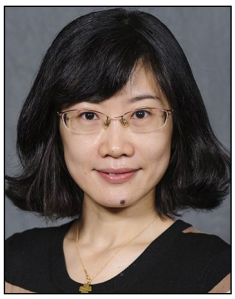

Lin Li is an associate professor at Arizona State University (ASU). She received her PhD degree from The Ohio State University, and has worked as a postdoctoral associate at the Massachusetts Institute of Technology. Prior to joining ASU, she was a faculty member at The University of Alabama. Her research interests include the field of multiscale material mechanics modeling for structural materials. She is the recipient of the Ralph E. Powe Junior Faculty Enhancement Award and the US Air Force Summer Faculty Fellowship. Li can be reached by email at lin.li.10@asu.edu.

Qiang Zhu is an associate professor in physics at the University of Nevada, Las Vegas (UNLV). He received his PhD degree from Stony Brook University, The State University of New York, in 2013, and his BS degree from Beihang University, China, in 2007. In 2016, he joined the UNLV to lead a research group in computational materials discovery. He is the recipient of the National Science Foundation CAREER Award (2021), the US Department of Energy Early CAREER Award (2021), and the Barrick Scholar Award (2022). Zhu can be reached by email at qiang.zhu@unlv.edu.

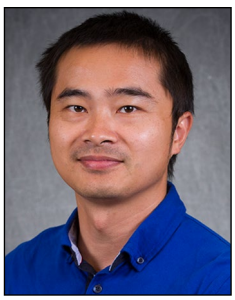

Houlong Zhuang is an assistant professor in the School for Engineering of Matter, Transport and Energy at Arizona State University. He obtained his doctorate in materials science and engineering from Cornell University in 2014. His current research is focused on applying quantum mechanical simulations, machine learning, and quantum computing calculations. He is a recipient of the National Science Foundation CAREER Award, Materials Today Rising Star Award, and the Talman Scholar Award in the 62nd Sanibel Symposium. Zhuang can be reached by email at zhuanghl@asu.edu.